

*Letter to Neuroscience*

## THE APICAL SHAFT OF CA1 PYRAMIDAL CELLS IS UNDER GABAERGIC INTERNEURONAL CONTROL

E. PAPP, X. LEINEKUGEL, D. A. HENZE, J. LEE and G. BUZSÁKI\*

Center for Molecular and Behavioral Neuroscience, Rutgers, The State University of New Jersey, 197 University Avenue, Newark, NJ 07102 New Jersey USA

*Key words:* inhibition, calcium spikes, spines.

**Dendrites of pyramidal cells perform complex amplification and integration (reviewed in Refs 5, 9, 12 and 20). The presence of a large proximal apical dendrite has been shown to have functional implications for neuronal firing patterns<sup>13</sup> and under a variety of experimental conditions, the largest increases in intracellular Ca<sup>2+</sup> occur in the apical shaft.<sup>4,8,15,16,19,21–23</sup> An important step in understanding the functional role of the proximal apical dendrite is to describe the nature of synaptic input to this dendritic region. Using light and electron microscopic methods combined with *in vivo* labeling of rat hippocampal CA1 pyramidal cells, we examined the total number of GABAergic and non-GABAergic inputs converging onto the first 200  $\mu\text{m}$  of the apical trunk. The number of spines associated with excitatory terminals increased from  $<0.2$  spines/ $\mu\text{m}$  adjacent to the soma to 5.5 spines/ $\mu\text{m}$  at 200  $\mu\text{m}$  from the soma, whereas the number of GABAergic, symmetric terminals decreased from 0.8/ $\mu\text{m}$  to 0.08/ $\mu\text{m}$  over the same anatomical region. GABAergic terminals were either parvalbumin-, cholecystokinin- or vasointestinal peptide-immunoreactive. These findings indicate that the apical dendritic trunk mainly receives synaptic input from GABAergic interneurons. GABAergic inhibition during network oscillation may serve to periodically isolate the dendritic compartments from the perisomatic action potential generating sites. © 2001 IBRO. Published by Elsevier Science Ltd. All rights reserved.**

From a larger database of biocytin-filled CA1 pyramidal cells labeled *in vivo*, 14 neurons with single apical trunks that lay favorably in the plane of focus were selected

(Fig. 1). Light microscopic examination of the proximal apical shaft revealed that not only the number of spines but also their morphology differed considerably from the spines on side and distal branches. For spines located on the main apical shaft, delineation of the border between spine head and neck was not always possible (Fig. 1C, D, F). This is in contrast to the side and distal branches where the spines have thin, long ( $>0.5 \mu\text{m}$ ) spine necks which are distinctly separate from the spine head (Fig. 1 E).

The spine density on the apical dendrite was similar to what has been described for *in vitro* labeled pyramidal cells.<sup>2</sup> The number of spines increased as a function distance from the soma. On average, the first spine appeared at  $39.4 \pm 12.7 \mu\text{m}$  from the soma. In the remaining part of the apical shaft, the number of spines increased almost linearly as a function of distance from the soma (Fig. 2A). No correction was made for spines obscured by the shaft and the distance was determined as a straight line along the dendrite.

For the determination of GABAergic inhibitory synapses on the apical shaft, post-embedding GABA immunostaining was performed on biocytin filled pyramidal cells. The proximal 200  $\mu\text{m}$  of the apical dendrites of two CA1 pyramidal cells were serially sectioned and reconstructed at the electron microscopic level (Fig. 3). Axon terminals with asymmetrical synapses on the head of spines served as a control for the determination of the non-specific background gold particle level used for GABA labeling (Fig. 3C, D). A bouton was considered GABA-positive if it showed a gold particle density at least five times that of the asymmetrical synaptic boutons (Fig. 3C, D, E). In the first pyramidal neuron, reconstructed from 250 ultrathin sections, 65 GABAergic and only two non-GABAergic synapses were found. Both non-GABAergic boutons established symmetrical synapses. No GABAergic terminals were found on spine heads or necks.<sup>7</sup> In the second neuron, reconstructed from 300 ultrathin sections, 52 GABAergic and two non-GABAergic synapses were found. One of the

\*Corresponding author. Tel.: +1-973-353-1080 ext. 3131; fax: +1-973-353-1820.

E-mail address: buzsaki@axon.rutgers.edu (G. Buzsáki).

Abbreviations: ABC, avidin–biotinylated horseradish peroxidase complex; CB, calbindin; CCK, cholecystokinin; DAB, 3,3'-diaminobenzidine; GluR, glutamate receptor; IP3, inositol triphosphate; NMDA, N-methyl-D-aspartate; PB, phosphate buffer; PV, parvalbumin; TBS, Tris-buffered saline; VIP, vasoactive intestinal polypeptide..

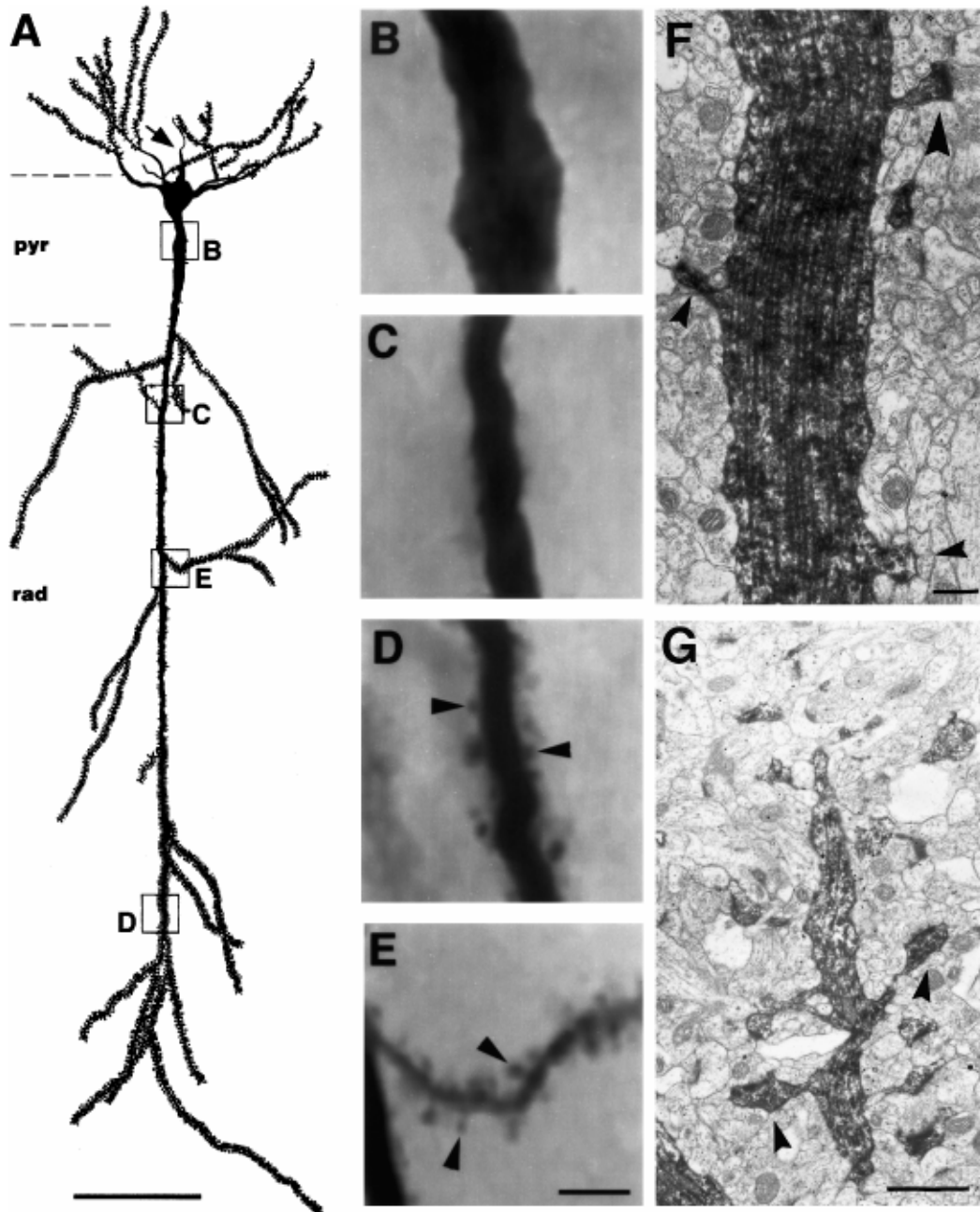


Fig. 1. Spine density on the apical shaft and side branches. (A) Camera lucida drawing of a biocytin-labeled CA1 pyramidal cell *in vivo*. Not all dendrites are shown. Boxed areas (A–E) are shown at higher magnification on the right. Arrow, axon. Arrowheads, spines. Note long spine necks on side branches (E) and the near absence of long-neck spines on the apical shaft (D). (F, G) Electron microscopic pictures of spines (arrowheads) on the apical shaft (F) and a side branch (G), approximately corresponding to locations D and E on panel A. Scale bars = 50  $\mu\text{m}$  (A); 5  $\mu\text{m}$  (B–E); 1  $\mu\text{m}$  (F–G)

immuno-negative boutons formed an asymmetrical synapse whereas the other was judged to be symmetrical. The number of GABAergic synapses observed on both of the apical dendrites gradually decreased as a function of distance from the soma (Fig. 2B). The size of most GABAergic boutons varied between 0.5 and 1.0  $\mu\text{m}$ . They contained rounded vesicles that were smaller than those observed in non-GABAergic boutons.<sup>7</sup> Occasionally, larger terminals (1–2.5  $\mu\text{m}$ ) were also observed in the vicinity of the soma (within 50  $\mu\text{m}$ ).

To further characterize the cellular origin of these

GABAergic boutons, immunostaining for vasoactive intestinal peptide (VIP), cholecystikinin (CCK), parvalbumin (PV) or calbindin (CB) was performed on 10 biocytin-labeled cells. In additional experiments, CA1 pyramidal cells were labeled with CB or glutamate receptor subunit (GluR) 2/3 antibodies<sup>11</sup> and then combined with VIP, CCK, PV or CB immunolabeling. In agreement with previous studies,<sup>1,7</sup> VIP, CCK and PV positive terminals were present on both the somata and proximal dendrites of pyramidal cells (Fig. 4). The density of PV immunostaining was much higher in the

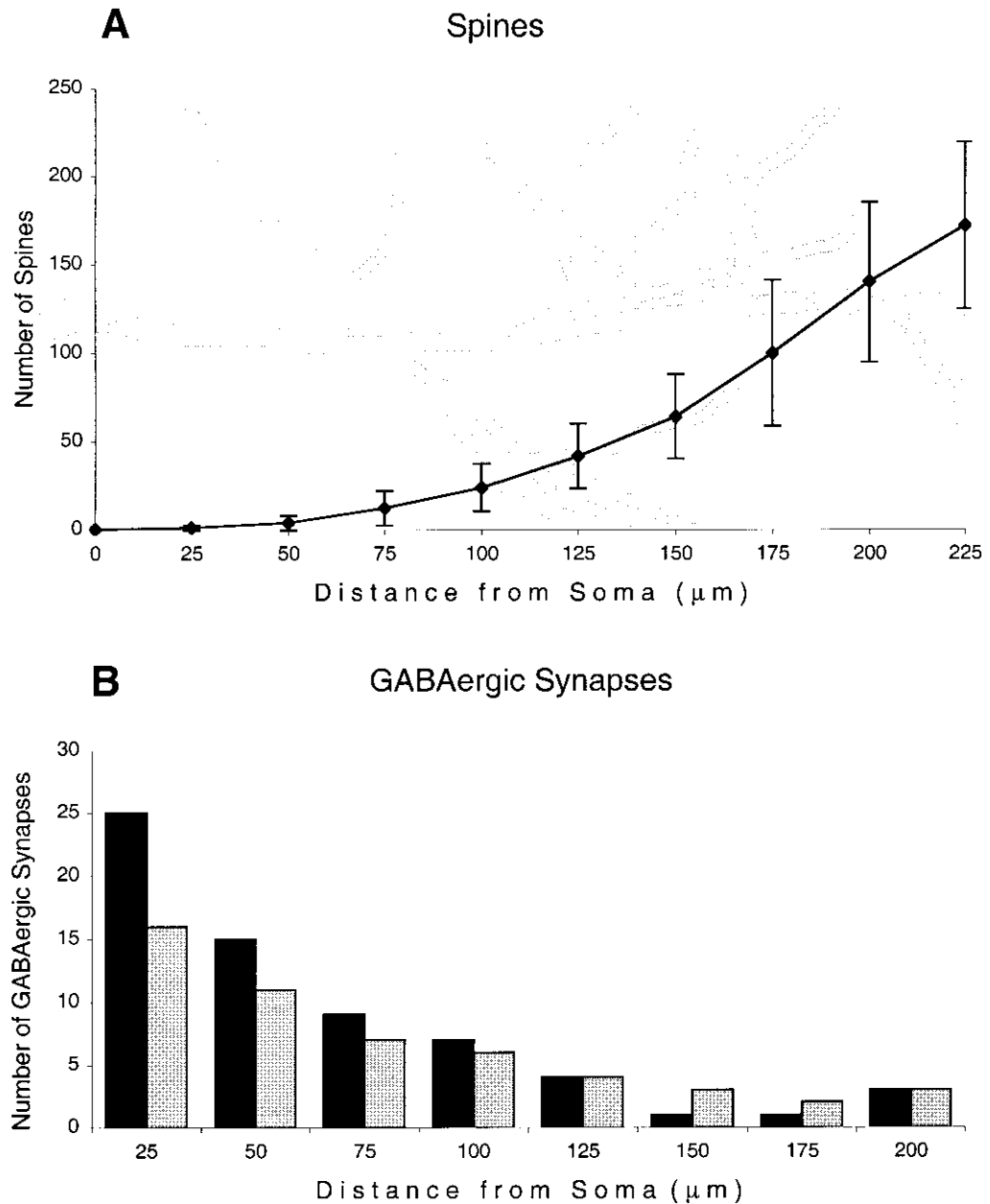


Fig. 2. Excitatory and inhibitory innervation of the apical dendritic shaft. (A) Total number of spines in 25- $\mu\text{m}$  segments from soma (mean  $\pm$  S.D.;  $n = 14$  cells). (B) Total number GABAergic synapses in 25- $\mu\text{m}$  segments from soma, as determined from two serially reconstructed neurons (black and gray columns) at the electron microscopic level. Note the reciprocal relationship between the number of spines and GABAergic terminals on the apical shaft.

pyramidal layer than in the stratum radiatum, whereas this difference was less expressed with VIP and CCK staining.

Our findings show that the apical shaft of CA1 pyramidal neurons is under a strong inhibitory control. The ratio of excitatory to inhibitory inputs increased from zero at the soma to 0.8 and 3.9 at 50  $\mu\text{m}$  and 100  $\mu\text{m}$  from the soma, respectively. These observations suggest that the physiological role of the apical shaft is fundamentally different from second and higher order dendrites. The proximal shaft is in many ways similar to the soma. It is well known that the soma receives primarily inhibitory synaptic input.<sup>6</sup> While the somatic

inhibition is believed to play a role in controlling action potential initiation at the axonal initiation site, the strong inhibitory control of the proximal apical dendrite may specifically modulate the communication between the soma and the apical dendritic tree. During the theta-associated coordinated increase of basket cell discharge, the input impedance of pyramidal neurons may decrease as much as 40%.<sup>10</sup> The rhythmic inhibitory shunting should physically change the electronic length<sup>3</sup> of the neuron and modulate the influence of apical dendritic excitatory inputs on the action potential initiation site in the axon.<sup>20</sup> Furthermore, by controlling the communication between somatic and dendritic compartments,

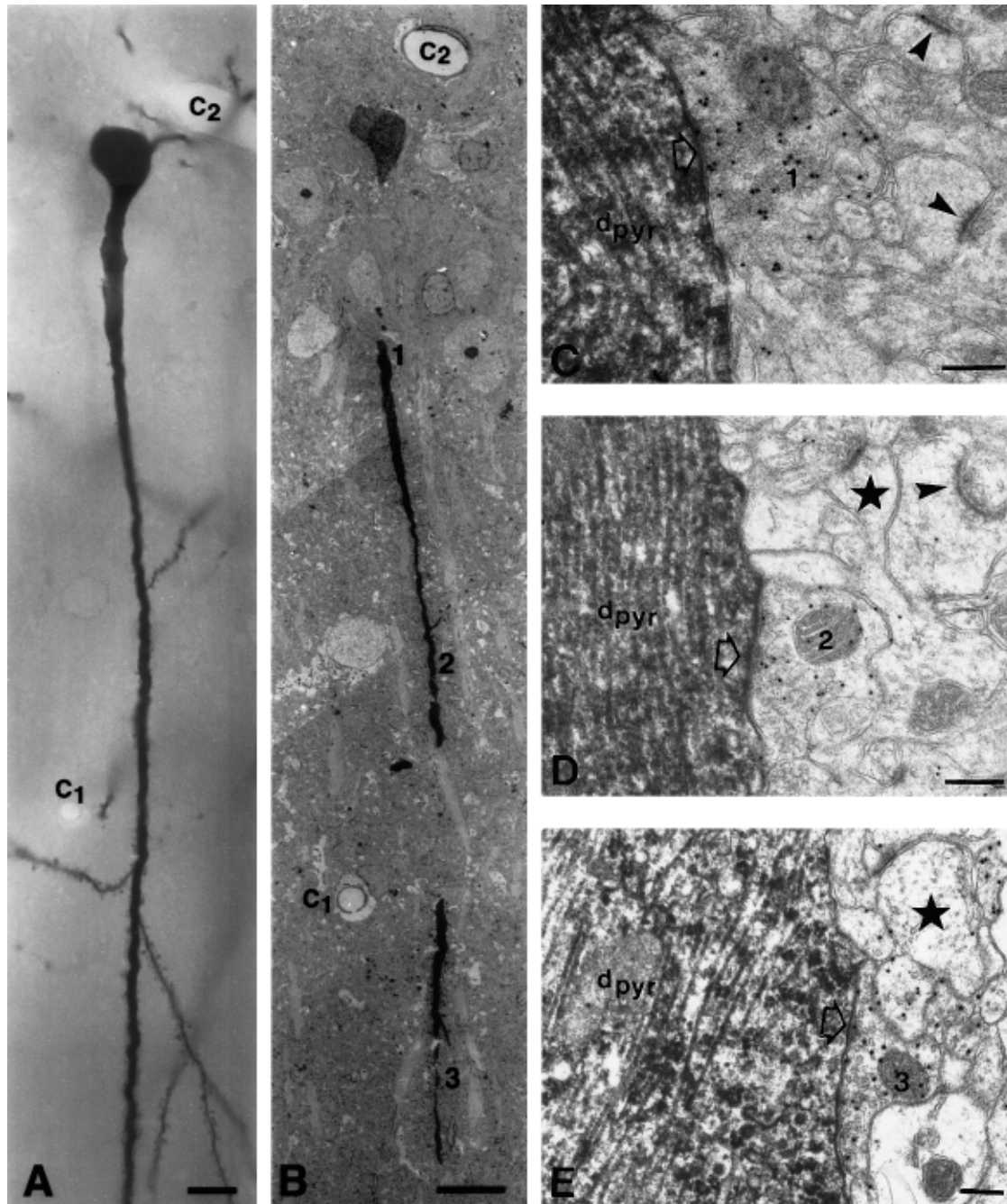


Fig. 3. Inhibitory innervation of the apical dendritic shaft. (A) Biocytin-labeled pyramidal cell. (B) Low-magnification electron microscopic picture of a thin section derived from the 60- $\mu\text{m}$  stained section in A. C1 and C2, capillaries. GABAergic synapses (1, 2 and 3) are shown at higher magnification (C, D, E). Note high density of gold-particles and mitochondria in these inhibitory synapses. Large arrows, postsynaptic density. Note also the low incidence of gold-particles in a spine (star in D) and dendrite (star in E). Arrowheads in C and D, non-GABAergic synapses. Dpyr, dendritic shaft of pyramidal cell. Scale bars = 10  $\mu\text{m}$  (A, B); 0.25  $\mu\text{m}$  (C–E).

inhibitory inputs to the apical trunk may modulate single spiking vs burst firing modes of pyramidal cells.<sup>13</sup>

Calcium imaging experiments *in vitro* consistently find a large  $\text{Ca}^{2+}$  influx in the proximal apical shaft of pyramidal neurons.<sup>4,8,15,16,19,21–23</sup> Large  $\text{Ca}^{2+}$  signals usually are explained by the activation of *N*-methyl-D-aspartate (NMDA) receptors, metabotropic glutamate receptors and/or voltage-sensitive  $\text{Ca}^{2+}$  channels (reviewed in Refs 5, 12 and 20). An important implication of these

findings is that under physiological conditions *in vivo*, large intracellular  $\text{Ca}^{2+}$  increases in the proximal apical dendrite are not directly mediated by activation of glutamate receptors in this region. Given the very low density of spines in the proximal part of the apical shaft, the role of synaptically activated NMDA receptors is likely to be minimal. Activity of proximal extrasynaptic NMDA and metabotropic glutamate receptors is also likely to be minimal due to the low overall density of glutamatergic

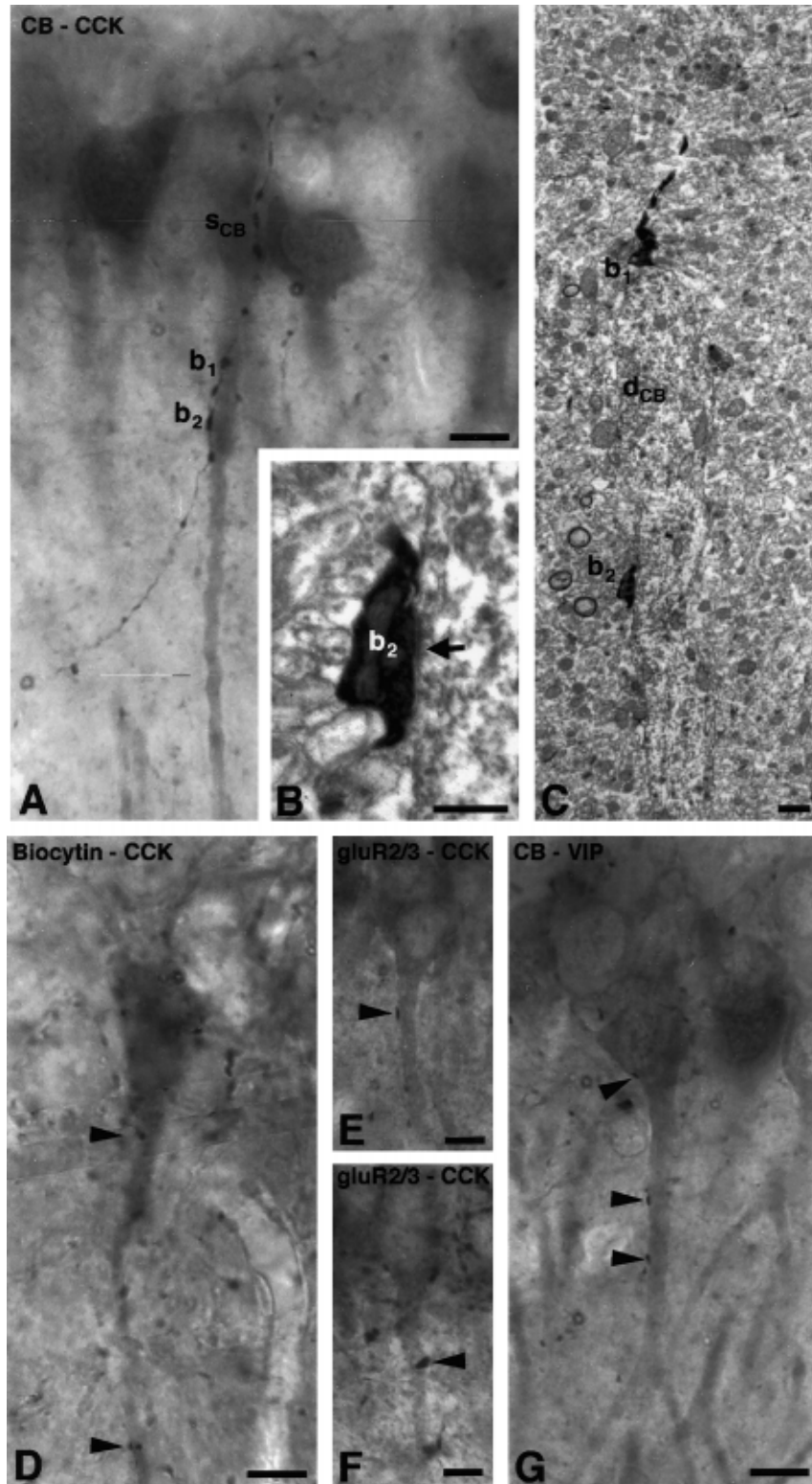


Fig. 4. Inhibitory innervation of the apical dendritic shaft. Double-stained immunosection for CCK (axon) and CB (pyramidal cell somata and dendrites).  $b_1$  and  $b_2$ , verified synapses, shown at higher magnification in B and C.  $s_{CB}$  and  $d_{CB}$ , calbindin-immunoreactive soma and dendrite, respectively. (D) CCK-immunoreactive boutons (arrowheads) on the apical shaft of a biocytin-labeled neuron. (E, F) CCK-immunoreactive boutons on dendrites of pyramidal cells labeled with GluR2/3 antibody. (G) VIP-immunoreactive boutons on the apical shaft of a CB-labeled pyramidal cell (arrowheads). Scale bars = 10  $\mu\text{m}$  (A, D–G); 0.5  $\mu\text{m}$  (B); 1  $\mu\text{m}$  (C).

terminals in the vicinity of the apical shaft. This reduced density of glutamatergic terminals suggests that the amount of extracellularly accumulating glutamate is probably lower than in the vicinity of more distal thinner branches. Therefore the high proximal intracellular  $\text{Ca}^{2+}$  signal is mediated either by voltage-sensitive calcium channels or intracellular  $\text{Ca}^{2+}$  stores. It has been shown that in the more proximal regions ( $<100 \mu\text{m}$  from the soma), the high-voltage activated L- and N-type  $\text{Ca}^{2+}$  channels occur at their highest density in the dendritic tree<sup>4</sup> and thus are likely to contribute to the  $\text{Ca}^{2+}$  signal. Other recent work has demonstrated that very strong activation of metabotropic glutamate receptors paired with backpropagating action potentials can lead to waves of intracellular  $\text{Ca}^{2+}$  being released from  $\text{IP}_3$  sensitive stores<sup>14</sup> suggesting that the intracellular  $\text{Ca}^{2+}$  stores also play an important role.

A final implication of these data is that the intracellular  $\text{Ca}^{2+}$  increases in the shaft are not likely to modulate glutamatergic receptors. Given the high density of GABAergic boutons in this region, we hypothesize that the large  $\text{Ca}^{2+}$  signal in the apical trunk serves to modulate GABAergic synaptic transmission by either potentiating or depressing GABA receptor responses.

#### EXPERIMENTAL PROCEDURES

The surgical and recording methods have been described in detail previously.<sup>17</sup> In short, adult Sprague–Dawley rats (200–300 g; Hilltop Laboratories, Scottsdale, PA) were anesthetized with urethane (1.5 g/kg; Sigma, St. Louis, MO, USA) and placed in a stereotaxic apparatus. A small (1.2 × 1.2 mm) bone window was drilled above the hippocampus (centered at AP = −3.5 and L = 2.5 mm from bregma) for intracellular recordings. The micropipettes were filled with 1 M potassium acetate and 1% biocytin (Sigma). *In vivo* electrode impedances were between 60 and 110 MΩ. All procedures were conducted in accordance with the NIH Guide for Care and Use of Laboratory Animals and were fully approved by the Rutgers Institutional Animal Care, which complies with federal and state laws. All efforts were made to minimize the number of animals used and their suffering.

Two to six hours after the intracellular biocytin injection, the animals were given an overdose of urethane and then perfused intracardially with physiological saline followed by 400 ml of fixative containing 4% paraformaldehyde, 0.2% picric acid, 0.05% glutaraldehyde in 0.1 M phosphate buffer (PB; fixative A); or 2% paraformaldehyde, 0.2% picric acid, 1% glutaraldehyde in 0.1 M PB (fixative B); or 5% acrolein (Sigma) in 0.1 M PB (fixative C). The brains were removed and coronal sections (60 μm) from the hippocampus were cut on a Vibroslicer (Ted Pella). Following extensive washes, the sections were immersed

in a cryoprotective solution (25% sucrose, 10% glycerol, in 0.01 M PB) and freeze-thawed three times over the surface of liquid nitrogen. The sections from animals perfused with fixative B or C, were treated with 1% NaBH<sub>4</sub> for 30 min. After repeated washes, first in 0.1 M PB and then Tris-buffered saline (TBS; pH 7.4) the sections were incubated in avidin–biotin–horseradish peroxidase complex (ABC, Vector Laboratories, Burlingame, CA; 1.5 h, 1:150) Biocytin labeling was visualized by 3,3'-diaminobenzidine-4HCl (DAB; Sigma) as a chromogen, which resulted in a brown reaction product. The sections were then treated with 1% OsO<sub>4</sub> in 0.1 M PB for 1 h, dehydrated in ethanol and propylene oxide, and embedded in Durcupan (ACM, Fluka, Neu Ulm, Germany). Serial ultrathin sections were cut with a Reichert ultramicrotome and examined with a Philips CM10 electron microscope.

For the examination of the peptide content of the synaptic input to the non-biocytin-filled CA1 pyramidal cells, first the neuron was visualized by Vector VIP substrate kit for peroxidase reaction (Vector Laboratories), which resulted a purple reaction product. Next, the sections were incubated in 10% normal goat serum (NGS) for 45 min followed by rabbit anti-CCK (1:8000), anti-VIP (1:8000), or parvalbumin (1:1000) for two days. This was followed by incubation in biotinylated-anti rabbit IgG (Vector Laboratories, 1:200), and ABC (1:150, Vector Laboratories). The immunoperoxidase reaction was developed with DAB as a chromogen, resulting in a brown reaction product. The slices were mounted on an object slides in DPX, coverslipped, or dehydrated in ethanol and propylene-oxide and embedded in Durcupan.

For double immunocytochemistry, the sections were first incubated in rabbit anti-CCK, anti-VIP and anti-PV and then biotinylated-anti rabbit IgG (Vector Laboratories, 1:200) followed by ABC (Vector Laboratories, 1:150). The sections were developed by ammonium-nickel sulphate-intensified DAB as a chromogen, which gave a black reaction product. The anti-calbindin and anti-GluR2/3 were used next, following the same procedure as above with biotinylated goat-anti-rabbit ABC, but only DAB was used to result in brown reaction product. The sections were dehydrated in ethanol and propyleneoxide and embedded in Durcupan.

From the material perfused with fixative B, ultrathin sections were cut and mounted on nickel grids and postembedding GABA immunostaining was carried out. The steps were made on droplets of solutions in humid Petri dishes as described earlier.<sup>18</sup> Low-magnification (×6600) images were taken from every 20th section using a Philips CM 10 electron microscope. The indentation between the soma and the apical trunk was used to determine the beginning of the dendritic shaft.

*Acknowledgements*—We thank T. F. Freund for his comments, E. Bonder for technical support, K. G. Baimbridge, T. Gorscs, and P. Somogyi for supplying us CB, PV, VIP, CCK and GABA antibodies, respectively. This work was supported by NIH (NS34994, MH54671), MH12403 (D.A.H.), Human Frontier Science Program (X. L.) and Soros Fellowship (E. P).

#### REFERENCES

1. Acsády L., Görös T. J. and Freund T. F. (1996) Different populations of vasoactive intestinal polypeptide-immunoreactive interneurons are specialized to control pyramidal cells or interneurons in the hippocampus. *Neuroscience* **73**, 317–334.
2. Bannister N. J. and Larkman A. U. (1995) Dendritic morphology of CA1 pyramidal neurones from the rat hippocampus: II. Spine distributions. *J. comp. Neurol.* **360**, 161–171.
3. Bernander O., Douglas R. J., Martin K. A. and Koch C. (1991) Synaptic background activity influences spatiotemporal integration in single pyramidal cells. *Proc. natn. Acad. Sci. USA* **88**, 11,569–11,573.
4. Christie B. R., Eliot L. S., Ito K., Miyakawa H. and Johnston D. (1995) Different  $\text{Ca}^{2+}$  channels in soma and dendrites of hippocampal pyramidal neurons mediate spike-induced  $\text{Ca}^{2+}$  influx. *J. Neurophysiol.* **73**, 2553–2557.
5. Eilers J. and Konnerth A. (1997) Dendritic signal integration. *Curr. Opin. Neurobiol.* **7**, 385–390.
6. Freund T. F. and Buzsáki G. (1996) Interneurons of the hippocampus. *Hippocampus* **6**, 347–470.
7. Gulyás A. I., Megias M., Emri Z. and Freund T. F. (1999) Total number and ratio of excitatory and inhibitory synapses converging onto single interneurons of different types in the CA1 area of the rat hippocampus. *J. Neurosci.* **19**, 10,082–10,097.
8. Jaffe D. B., Johnston D., Lasser-Ross N., Lisman J. E., Miyakawa H. and Ross W. N. (1992) The spread of  $\text{Na}^+$  spikes determines the pattern of dendritic  $\text{Ca}^{2+}$  entry into hippocampal neurons. *Nature* **357**, 244–246.

9. Johnston D., Magee J. C., Colbert C. M. and Christie B. R. (1996) Active properties of neuronal dendrites. *A. Rev. Neurosci.* **19**, 165–186.
10. Kamondi A., Acsády L., Wang X. J. and Buzsáki G. (1998) Theta oscillations in somata and dendrites of hippocampal pyramidal cells in vivo: activity-dependent phase-precession of action potentials. *Hippocampus* **8**, 244–261.
11. Léránth C., Szeideemann Z., Hsu M. and Buzsáki G. (1996) AMPA receptors in the rat and primate hippocampus: a possible absence of GluR2/3 subunits in most interneurons. *Neuroscience* **70**, 631–652.
12. Magee J., Hoffman D., Colbert C. and Johnston D. (1998) Electrical and calcium signaling in dendrites of hippocampal pyramidal neurons. *A. Rev. Physiol.* **60**, 327–346.
13. Mainen Z. F. and Sejnowski T. J. (1996) Influence of dendritic structure on firing pattern in model neocortical neurons. *Nature* **382**, 363–366.
14. Nakamura T., Barbara J. G., Nakamura K. and Ross W. N. (1999) Synergistic release of  $\text{Ca}^{2+}$  from IP<sub>3</sub>-sensitive stores evoked by synaptic activation of mGluRs paired with backpropagating action potentials. *Neuron* **24**, 727–737.
15. Regehr W. G., Connor J. A. and Tank D. W. (1989) Optical imaging of calcium accumulation in hippocampal pyramidal cells during synaptic activation. *Nature* **341**, 533–536.
16. Sandler V. M. and Ross W. N. (1999) Serotonin modulates spike backpropagation and associated  $[\text{Ca}^{2+}]_i$  changes in the apical dendrites of hippocampal CA1 pyramidal neurons. *J. Neurophysiol.* **81**, 216–224.
17. Sik A., Penttonen M., Ylinen A. and Buzsáki G. (1995) Hippocampal CA1 interneurons: an *in vivo* intracellular labeling study. *J. Neurosci.* **15**, 6651–6665.
18. Somogyi P. and Hodgson A. J. (1985) Antisera to gamma-aminobutyric acid. III. Demonstration of GABA in Golgi-impregnated neurons and in conventional electron microscopic sections of cat striate cortex. *J. Histochem. Cytochem.* **33**, 249–257.
19. Spruston N., Schiller Y., Stuart G. and Sakmann B. (1995) Activity-dependent action potential invasion and calcium influx into hippocampal CA1 dendrites. *Science* **268**, 297–300.
20. Stuart G., Spruston N., Sakmann B. and Häusser M. (1997) Action potential initiation and backpropagation in neurons of the mammalian CNS. *Trends Neurosci.* **20**, 125–131.
21. Svoboda K., Denk W., Kleinfeld D. and Tank D. W. (1997) *In vivo* dendritic calcium dynamics in neocortical pyramidal neurons. *Nature* **385**, 161–165.
22. Tsubokawa H. and Ross W. N. (1996) IPSPs modulate spike backpropagation and associated  $[\text{Ca}^{2+}]_i$  changes in the dendrites of hippocampal CA1 pyramidal neurons. *J. Neurophysiol.* **76**, 2896–2906.
23. Yuste R., Gutnick M. J., Saar D., Delaney K. R. and Tank D. W. (1994)  $\text{Ca}^{2+}$  accumulations in dendrites of neocortical pyramidal neurons: an apical band and evidence for two functional compartments. *Neuron* **13**, 23–43.

(Accepted 14 December 2001)